Detection of large-scale climate signals in spring vegetation index (normalized difference vegetation index) over the Northern Hemisphere

Dao-Yi Gong

Key Laboratory of Environmental Change and Natural Disaster, Institute of Resource Science, Beijing Normal University, Beijing, China

School of Earth and Environmental Sciences, Seoul National University, Seoul, South Korea

Chang-Hoi Ho

School of Earth and Environmental Sciences, Seoul National University, Seoul, South Korea

Received 13 March 2002; revised 15 February 2003; accepted 24 March 2003; published 20 August 2003.

[1] Climate is one of the determinants driving ecosystems on both local and global scales. During the last two decades, there has occurred a dramatic temperature increase in the northern midlatitudes to high latitudes. The rapid warming has resulted in the promotion of bioactivity and an early growing season. However, the temperature and vegetation changes are not uniform in geographical distribution. In the present study, we analyze the spatial features in the normalized difference vegetation index (NDVI)-temperature relationship over Eurasia and North America in spring for the period 1982–2000. The NDVI data are derived from the Earth Observing System Pathfinder advanced very high resolution radiometer data sets. A singular value decomposition analysis is applied to the covariance matrix of the NDVI and temperature. Most of the squared covariance, 91.6%, is captured by the first seven paired modes. The result clearly indicates that the temperature is a focal factor influencing vegetation activity. Furthermore, those seven paired modes show large-scale features and well-defined patterns. The atmospheric circulation systems, such as the Southern Oscillation, North Atlantic Oscillation/Arctic Oscillation, Pacific/North American pattern, Eurasian pattern, western Pacific pattern, western Atlantic pattern, eastern Atlantic pattern, and North Pacific index, are found to be associated with that. The time coefficient corresponding to the first paired modes, centered on western Siberia, is correlated significantly with the Eurasian teleconnection pattern. Their correlation coefficients are 0.72 and 0.78 for vegetation and temperature, respectively, for the data period. Other modes are also correlated with one or more circulation indices. This implies that the large-scale circulation is essential for understanding the regional response of vegetation to global climate change. Taking all nine circulation indices and time lags into account, a large portion (71%) of the satellite-sensed variance in NDVI could be explained. The temperature-NDVI relationships did not change significantly when the NDVI was rescaled from 1 to 5 degrees, indicating that the singular value decomposition analysis is an appropriate technique for detecting the degree of coupling between vegetation and climate and that the vegetation-temperature relationship presented in this study is robust. *INDEX TERMS:* 0315 Atmospheric Composition and Structure: Biosphere/atmosphere interactions; 1610 Global Change: Atmosphere (0315, 0325); 1620 Global Change: Climate dynamics (3309); 1630 Global Change: Impact phenomena; 1640 Global Change: Remote sensing; *KEYWORDS:* normalized difference vegetation index, climate impact, atmospheric circulation, teleconnection, vegetation change

Citation: Gong, D.-Y., and C.-H. Ho, Detection of large-scale climate signals in spring vegetation index (normalized difference vegetation index) over the Northern Hemisphere, *J. Geophys. Res.*, *108*(D16), 4498, doi:10.1029/2002JD002300, 2003.

0148-0227/03/2002JD002300$09.00

1. Introduction

[2] There is increasing attention focused on the variations in global vegetation condition because of their

importance in the global carbon cycle [e.g., *Tans et al.*, 1990; *Myneni et al.*, 2001; *Keeling et al.*, 1996]. The vegetation variability arises from many causes. It is well known that climate drives ecosystems on both local and global scales. Vegetation change in response to the large-scale climate change is a challenging topic in global change study.

[3] To date, at least two climatic factors and their possible impact on vegetation activity are highlighted. One is global warming and the other is El Niño/Southern Oscillation (ENSO). A particularly impressive climate feature is that the global temperature has experienced a remarkable increase in the last about two decades or so. Since the late 1970s, the annual mean land-surface air temperature averaged over the Northern Hemisphere has been increasing at an unprecedented rate of 0.31°C per decade [*Intergovernmental Panel on Climate Change* (*IPCC*), 2001]. It is widely recognized that a warming climate could generally promote biological activity and therefore favor a higher vegetation index (such as the normalized difference vegetation index, hereafter NDVI). However, in some cases a higher temperature may induce drought stress if rainfall is a prominent control factor but does not increase at the same time [*Barber et al.*, 2000]. Many previous studies have reported that NDVI over midlatitude and high-latitude Eurasia and North America have also risen steadily since the early 1980s [e.g., *Myneni et al.*, 1998; *Kawabata et al.*, 2001; *Zhou et al.*, 2001; *Tucker et al.*, 2001]. A large portion of the enhanced vegetation activity would be attributed to the concurrent climate warming.

[4] However, both surface air temperature changes and vegetation variations are not uniform in terms of geographical distribution. For the regional to continental temperature variability over midlatitudes to high latitudes, fluctuations of such atmospheric circulation as the North Atlantic Oscillation/Arctic Oscillation (NAO/AO), Pacific/North American pattern (PNA), Eurasian pattern (EU), etc., would play important roles. These large-scale atmospheric circulations exert a direct and imperative influence on regional and continental climate. For example, it is found that the observed warming trends in North America are significantly related to atmospheric circulation fluctuations [*IPCC*, 2001]. *Hurrell* [1996] and *Thompson et al.* [2000] pointed out that the NAO/AO is probably a major cause of the cold-season warming in Siberia and northern Europe. Given the evident connection between temperature and atmospheric circulation, and between vegetation conditions and temperature, one would think that, in addition to botanical and local environmental factors, the large-scale atmospheric circulation should exert influence on vegetation conditions too. For example, *Los et al.* [2001] detected a significant NAO signal in NDVI in Europe.

[5] The purpose of the present research is to investigate the large-scale NDVI-temperature relationships, and to analyze the extent to which these NDVI-temperature relationships are associated with the changes in atmospheric circulation fluctuations. The target region in this study is limited to extratropical Eurasia and North America (north of 30°N). We analyze only the spring (April and May) NDVI since this is the season during which both temperature and NDVI have shown profound changes during the last two decades. Many studies have reported that spring has experienced stronger NDVI trends than other growing seasons [*Zhou et al.*, 2001].

[6] In section 2 we discuss the data and investigative method. The coupling patterns between NDVI and temperature, sensitivity of NDVI to temparature, NDVI trends, and the correlation between NDVI and large-scale climate indices are presented in section 3. Discussions on the independence of NDVI-temperature relationships with respect to the spatial resolution of the data, on the influence of ENSO on NDVI, and on the influence of data errors are presented in section 4. Section 5 summarizes the results.

2. Data and Method

2.1. NDVI

[7] The NDVI data derived from the advanced very high resolution radiometer (AVHRR) on the National Oceanic and Atmospheric Administration (NOAA) polar-orbiting satellite is widely used as an indicator of the vegetation activity [*Tucker and Sellers*, 1986]. The AVHRR NDVI data used in the present study are produced by the NOAA/NASA Earth Observing System Pathfinder AVHRR Land Program and are available from the NASA Goddard Space Flight Center Distributed Active Archive Center via the Internet at http://eosdata.gsfc.nasa.gov. Further details of the data set are given by *James and Kalluri* [1994] and *Agbu and James* [1994]. We use NDVI in two forms, one is the real value, and the other is the anomaly with respect to the entire period 1982–2000. The seasonal mean is averaged for April to May at each cell.

[8] High-resolution NDVI data are usually affected by many environmental variables on both local and regional scales, leading to a very high variability in both temporal and spatial domains. Regional averaging can efficiently reduce or suppress the high-frequency noise. Since our objective is to examine the large-scale temperature-NDVI relationship, we use the coarser monthly 1°longitude × 1°latitude data sets rather than the higher resolution of 4 km or 8 km data sets. However, it should be noted that the 1 degree Pathfinder data contains significant cloud effects due to the nonremoval of clouds prior to averaging the 4 or 8 km data to 1 degree. Stratosphere aerosol output by major volcanic eruption also affects the AVHRR data, including the NDVI. Some studies stated that correction to NDVI errors due to the El Chichon and Mount Pinatubo volcanic eruptions notably improve the data quality, particularly in the tropical areas [*Zhou et al.*, 2001]. All these factors result in systematic errors in the NDVI production. In section 4.3 we discuss the influence of Pathfinder data errors on NDVI-temperature relations in detail.

2.2. Temperature

[9] A land surface air temperature data set on a 5°longitude × 5°latitude grid is utilized in the present study. The observed station temperature data in the form of anomalies from the 1961–1990 base period is collected and interpolated to a regular set of grid boxes, finally resulting in the data set [*Jones*, 1994]. We use only the data for the period 1982–2000 coincident with the same time span of NDVI. Thus the temporal average of temperature at each box for the period 1982–2000 is usually not zero. To facilitate the computation of covariance and sub-

sequent analysis, the 1982–2000 means are subtracted from the monthly values of each year for each box.

2.3. Atmospheric Circulation Indices

[10] Atmospheric circulation indices used include the Southern Oscillation Index (SOI), NAO, AO, EU, PNA, the western Pacific (WP) pattern, the western Atlantic (WA) pattern, the eastern Atlantic (EA) pattern, and the North Pacific (NP) index. SOI is the standardized sea level pressure difference between Tahiti and Darwin, obtained from the Climate Prediction Center, National Centers for Environmental Prediction (NCEP), NOAA. NAO is the difference of normalized sea level pressures (SLP) between Azores and Iceland [*Hurrell*, 1995]. AO is obtained from *Thompson and Wallace* [1998]. The EU, WP, WA, PNA and EA indices are derived from the formula given by *Wallace and Gutzler* [1981] by employing the NCEP/NCAR (National Center for Atmospheric Research) reanalysis 500 hPa height data. The NP Index is the area-weighted sea level pressure over the region 30°–65°N, 160°E-140°W [*Trenberth and Hurrell*, 1994]. All of these indices are monthly. The 19 springs (April–May) from 1982 to 2000 are considered here. The locations of the index centers and their polarities for seven indices are demonstrated in Figure 1.

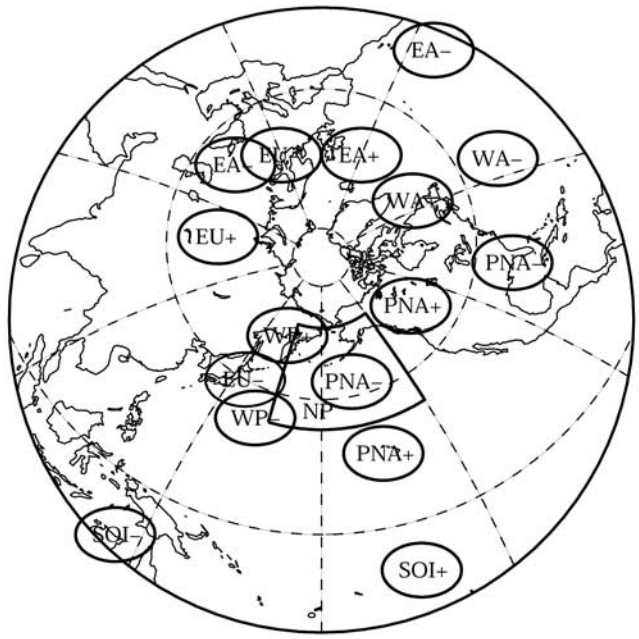

Figure 1. Locations of the index centers for SOI, EU, WP, WA, PNA, and EA. The polarity of each center corresponding to a positive index condition is also demonstrated. Centers for NAO and AO have not shown for simplicity.

2.4. Method

[11] To reveal the spatial-temporal characteristics rooted in the vegetation activity, the empirical orthogonal function (EOF)/principal component analysis (PCA) is usually applied to the NDVI data. It can detect the spatial-temporal features embedded in the data set. However, the disadvantage is that the detected leading modes may be nonclimate induced or even nonvegetation related in some circumstances. In the present study, we apply the singular value decomposition (SVD) analysis to NDVI and temperature. This technique is suited for resolving such problem as the association between two different geophysical variables. The procedure is described briefly as follows.

[12] Given two matrices A and B, the elements of $A_{L\times M}$ are temperature at M different spatial cells and L different times. The elements of matrix $B_{L\times N}$ are NDVI at N locations with the same time domain (L). Both A and B at each location are anomalies with respected to the entire time period, having zero mean. The covariance matrix $C_{M\times N}$ is formed from $A_{L\times M}$ and $B_{L\times N}$: $C = (1/L)A^TB$. Then the SVD on the covariance matrix C is carried out, finally, yielding the following: (1) A set of singular values, Σ. Since the sum of the squares of the singular values is equal to the total squared covariance between all the elements of the temperature and NDVI, so each singular value indicates the relative importance of the corresponding spatial modes. (2) Pairs of mutually orthogonal patterns defined by the matrices U and V, where, $C = U\Sigma V^T$. (3) Corresponding expansion time-coefficients X = AU and Y = BV. For the special case in which A and B is the same matrix, SVD analysis is equivalent to EOF analysis. The SVD is often utilized to identify the degree of coupling between two geophysical variables [e.g., *Wallace et al.*, 1992; *Bretherton et al.*, 1992].

[13] Of great importance is that the leading paired modes between NDVI and temperature are the largest signal involved between them in both time and space domains, and the relationships as revealed by the leading modes are in general of the large-scale connections rather than of the local phenomena.

3. Results

3.1. Coupling Patterns Between NDVI and Temperature

[14] We discard the cells where the NDVI data are not available for more than 2 years in the entire 19-year period from 1982 to 2000 (L = 19). There are 8775 cells in total remained, i.e., M = 8775. The result for temperature is 264 in the same spatial domain, i.e., N = 264. We put NDVI and temperature anomalies into matrices A and B, respectively, then perform SVD analysis, and finally obtain the results. It is important to note that the NDVI and temperature are of different units. Given the fact that normalization of NDVI will largely bias the variance to the small-NDVI-value regions, and produce huge errors in some regions where the mean NDVI values near zero. And the scaling of temperature will also smooth the spatial difference of the variance, decreasing the importance of middle latitude climates artificially. To avoid these we do not normalize both variables prior to analysis.

[15] As indicated in the previous section, the singular value is an indicator of the importance of the corresponding modes concerning the NDVI-temperature squared covariance, and therefore also a measurement of the degree of association between the NDVI and temperature. As the singular values drop off monotonically with the mode number, the importance of the paired modes also decreases steadily. The explained squared covariances are highly concentrated in the first several modes, with the first seven contributing more than 91% of the total amount. That means

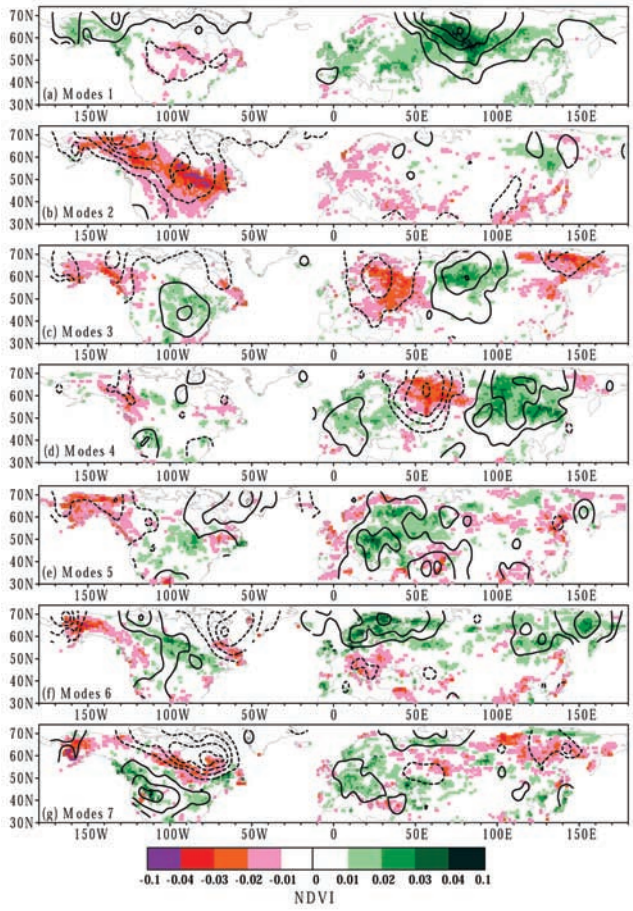

Figure 2. First seven paired modes of NDVI and temperature. NDVI is shown in color. Temperature is shown in contours with interval 0.05; dashed lines indicate the negative values, solid the positive, zero contours are omitted for simplicity. Both units are arbitrary. Their corresponding time coefficients are shown in Figure 3.

there are strong relationships between the two fields and we would need to analyze only the several principal patterns, since most of the information regarding NDVI-temperature coupling has already been captured by them. The strength of the connection can also be seen in the tight correlations between the corresponding expansion time series for each paired mode. For the first seven paired modes, the correlations between NDVI and temperature expansion coefficients vary from 0.94 to 0.97.

[16] Figures 2 and 3 present the first seven coupled modes and their corresponding time coefficients. The separated large-scale centers, rather than randomly scattered spots, of both NDVI and temperature are most impressive. These centers of NDVI are also highly consistent with those of temperature; both are positive or negative at the same time, implying high positive sensitivity of NDVI to temperature over these centers. Many previous studies analyze the NDVI of the continental or zonal mean as a whole. As our figures shown, that would have smoothed out the most sensitive signals and underestimated the response of vegetation to temperature changes over these regions.

[17] The most important NDVI-temperature connection exists in high-latitude Eurasia, centered on Siberia. This mode accounts for 42.6% of the total squared covariance between NDVI and temperature. The second mode, which accounts for 19.5%, indicates a coherent vegetation-temperature relationship over North America with the center located in the middle to eastern United States. Both modes 1 and 2 are of continental scale. The third and fourth modes show some predominant regional patterns. The importance of the fifth and other modes are relatively low, and they show more scattered centers, particularly for the NDVI.

[18] It is interesting to note that remarkable association occurs over some rather confined regions, for instance, Siberia, the mideastern United States, eastern Europe, and Alaska. This suggests that the response of NDVI to temperature may be geographically locked in association with the regional patterns of temperature changes. We will display in the following section that these inherent temperature modes are, to a large extent, due to the large-scale atmospheric circulation fluctuations.

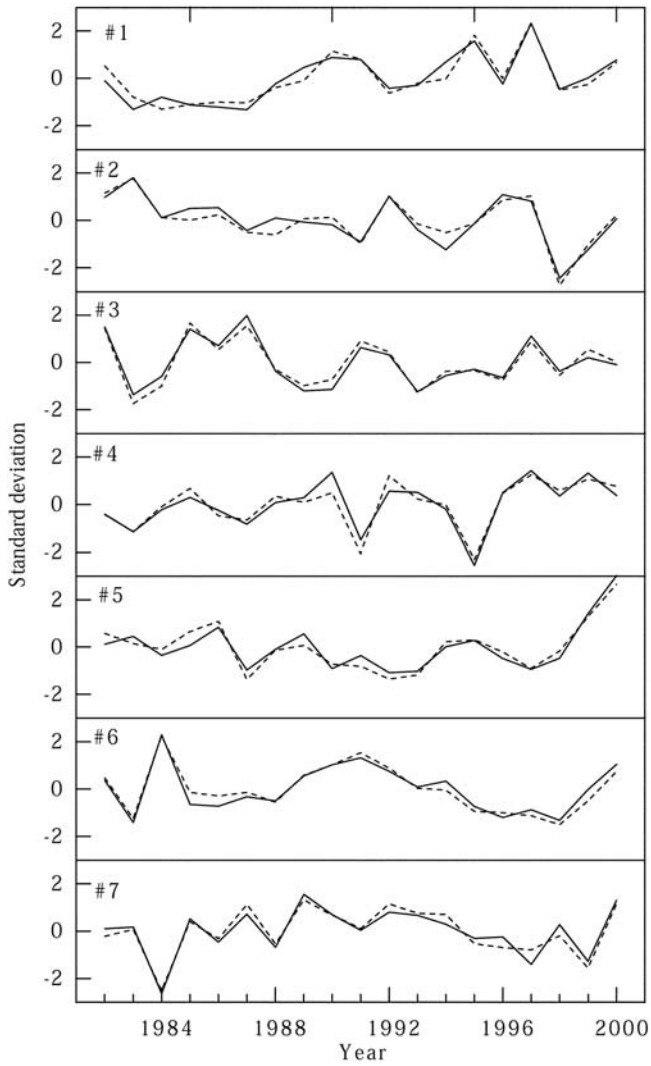

Figure 3. Corresponding time coefficients for the first seven paired modes. Solid lines are for NDVI, and dashed lines for temperature. All normalized.

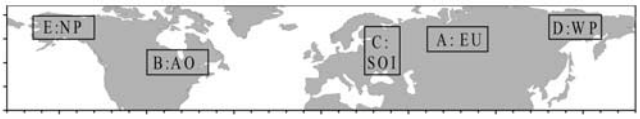

Figure 4. Several key regions showing strong association between NDVI and temperature. These regions are also considered in detail for investigation of relationship between NDVI and the large-scale atmospheric circulation changes. Shown in each box is the climate index with highest correlation to regional NDVI. See Table 2 for details.

[19] The expansion time coefficients of SVD modes are not mutually orthogonal, though the correlations between them tend to be small. Our results show that the simultaneous correlation among nonpaired expansion time series are small and none of them significant. In addition, there are possibilities that the lagged climate signals might show up in different NDVI modes. In other words, it is possible that several of these modes are paired and are a manifestation of the same climate signal. To clarify these, we compute the autocorrelation of expansion time series of temperature with lag varying from zero to 5 years. Results show that there are no significant lags in temperatures modes. That implies that the NDVI modes detected by SVD analysis refer to different temperature signals.

3.2. Sensitivity of NDVI to Temperature

[20] To identify the possible connection of NDVI to large-scale temperature, the correlation coefficients between NDVI and temperature are calculated. Several key regions are considered. These regions are selected as the strongest coupling centers as Figure 2 reveals. They are regions (A) West Siberia, 55°–65°N by 60°–95°E, (B) Middle North America, 45°–55°N by 65°–100°W, (C) East Europe, 45°–65°N by 25°–45°E, (D) Northeast Asia, 60°–70°N by 130°–160°E, and (E) Northwest North America, 60°–70°N by 130°–165°W. See Figure 4 for their locations. In addition to these centers, the statistics for North America in 40°–70°N, Eurasia in 40°–70°N and the entire Northern Hemisphere in 40°–70°N are also carried out for comparison. The ordinary linear regression analysis is utilized for the NDVI and temperature series for these regions. The relationships are determined, and shown in Table 1. Note that West Siberia and Middle North America display the most significant relationships (the correlation coefficients are 0.89 and 0.84, respectively). Not surprisingly, that is in well agreement with the results of SVD analysis since these two regions appear as the centers of the first two leading modes. All of the NDVI-temperature relations are statistically significant at the 95% confidence level. That is the well-known notion of the positive relationship, i.e., a warmer spring would promote the vegetation activity, lengthen the growing season, and thus result in higher biomass productivity [e.g., *Zhou et al.*, 2001; *Myneni et al.*, 2001]. Note that for East Europe and Northeast Asia, the correlation with temperature is not as significant as for the others, though it also exceeds the confidence level. This might be due to some other factors such as the rainfall, and/or cloud amount, etc. This aspect needs further investigation.

3.3. NDVI Trend

[21] As can be seen in Figure 3, the time coefficients of leading modes display evident trends. That suggests there are long-term changes in NDVI over the center regions corresponding to those modes. The time series and ordinary linear trends of spring NDVI in these regions are presented in Figure 5. From 1982 to 2000, NDVIs in all analyzed regions show upward trends. The most remarkable trend occurs in the northwestern North America (23.9%/10 years). The second highest value is 17.9%/10 years, for West Siberia. On the other hand, there is no evident increase in northeastern Asia (1.1%/10 years). However, only three NDVI trends in East Europe, Eurasia, and the entire northern high latitudes are statistically significant at the 95% confidence level. Although the average NDVI for 40°–70°N are increasing significantly, the two sub-continents do not show the same changes. The increase in NDVI in North America is neither as large as in Eurasia nor as significant. Some other studies also reported the similar results showing a difference between the two continents [e.g., *Bogaert et al.*, 2002].

[22] Using different NDVI data sets, *Zhou et al.* [2001] found that the absolute and percent NDVI changes are largest during spring in both North America and Eurasia. They indicated that NDVI trends for 40°–70°N in Eurasia and North America from 1982 to 1999 in April to May are 20.87% and 16.84%, respectively, both the highest in all growth seasons in the two continents. After transformation to percentage per decade, the two values are almost the same as our results, though they take only vegetated pixels with 8 km resolution into account.

[23] Notice that both the strongest and weakest trends occur in the sub-polar regions, namely, Northeast Asia and Northwest North America. Both regions are sparsely vegetated areas, the average NDVI in them in April–May are only 0.07 and 0.12, respectively. Caution is advisable when explaining the changes there because the actual vegetation condition may be exacerbated by nonvegetation factors such as snow, ice and water in these high-latitude regions.

3.4. Correlation Between NDVI and Large-Scale Climate Indices

[24] The above sections show there are regional features in the sensitivity and trend of NDVI. The regional differ-

Table 1. Statistics for the Relationship Between NDVI and Temperature in Several Regions[a]

Region	Statistics		
	Regression	r	p
West Siberia	$V = 0.292 + 1.235T$	0.89	<0.0001
Middle N. America	$V = 0.346 + 1.232T$	0.84	<0.0001
East Europe	$V = 0.428 + 0.972T$	0.51	0.024
Northeast Asia	$V = 0.072 + 0.528T$	0.47	0.047
Northwest N. America	$V = 0.123 + 0.927T$	0.82	<0.001
N. America	$V = 0.1945 + 0.983T$	0.84	<0.0001
Eurasia	$V = 0.240 + 1.247T$	0.72	0.00045
40°–70°N	$V = 0.223 + 1.509T$	0.77	0.001

[a]Here, V, NDVI; T, temperature; r, correlation coefficient; and p, probability.

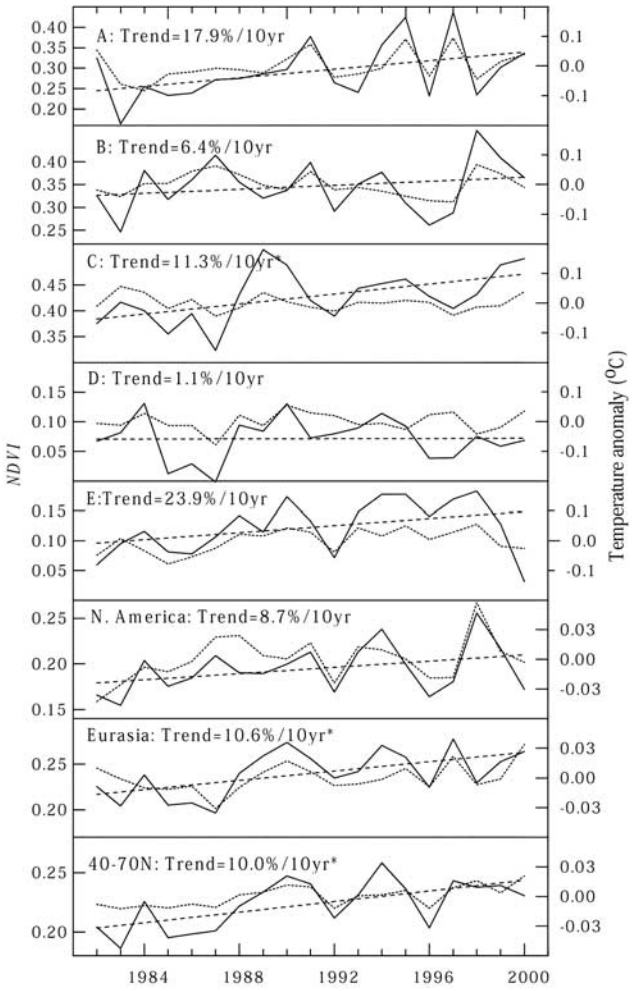

Figure 5. Time series of regional mean NDVI. Solid lines are absolute values of NDVI of each year. Dotted lines are temperature. Dashed lines are linear trends of NDVI. Trends statistically significant at the 95% confidence level are marked with asterisks. See Figure 4 for region locations.

ence may be partly due to the large-scale atmospheric circulation systems. In this section we investigate the possible connection between the regional NDVI and atmospheric indices. Table 2 presents the results. The connection between the regional NDVI and some atmospheric indices is significant, some is not. This might be due to the regional difference of the influence of these atmospheric circulation systems. One climate index would exert stronger influence over some confined regions than over others. Thus, for a specific region, the temperature and NDVI may correlate more significantly to one or more climate indices than to others. For West Siberia, the most important atmospheric system is EU. The correlation between NDVI and EU ($r = 0.81$) is the most significant among all values shown in Table 2. The EA also contributes much variance in NDVI since the correlation between them is 0.53. Comparison of the spatial patterns in atmospheric circulation and temperature associated respectively with the positive-phase EU and EA shows the same positive centers over Siberia. Taking both EU and EA into account, 69.4% of the variance in spring NDVI could be explained. For Middle North America AO/NAO exerts a larger influence on vegetation than the other factors. In East Europe, the SOI dominates over other indices. The influence of ENSO on temperature over eastern Europe is consistently significant ($r = 0.49$). The NDVI changes in Northeast Asia show no prominent connection with any indices, despite the temperature there being notably affected by the WP ($r = 0.67$). That may be partly due to the bad vegetation condition. Both PNA and NP indices are significantly correlated with NDVI in Northwest North America, the two together explaining 33.2% of the NDVI variance. These significant factors can also been seen in Figure 2 in the well-defined spatial features. For example, the WA pattern in paired mode 7 and the NAO pattern in paired mode 6 are clearly remarkable.

[25] Figure 6 depicts the scatterplots of the time coefficients of NDVI versus the most important factors associated with them. The fourth paired modes show no significant correlation with any index. This mode may be a combined pattern contributed by ENSO, WP, EU, and AO. They explain in total 24.1% of the variance of the NDVI time coefficient.

[26] However, when Eurasian and North American means are considered, these factors are no longer dominant. For the hemispheric mean averaged over 40°–70°N, none of the factors is significant above the confidence level and the hemispheric mean temperature also does not show significant correlation with any index. Our results imply that it might be more appropriate to focus on the regional rather than on the continental or hemispheric means when determining the impact of global climate change on the ecosystems because the continental and hemispheric means would smooth out the meaningful regional features.

[27] It is interesting to note that there are evident connection between Middle North America, as well as North America as a whole, and WP (correlation coefficient for Middle North America NDVI and WP is −0.37, for the whole of North America it is −0.42). The two centers used to define WP are located over the western Pacific (60°N, 155°E and 30°N, 155°E). How does this remote connection occur? *Wallace and Gutzler* [1981, Figure 24] showed that anomalies associated with WP in 500 hPa geopotential heights extend from the North Pacific to the midlatitudes along the western coast of North America. We calculate the correlation coefficient between WP and 500 hPa height over the Northern Hemisphere in 1982–2000 for April to May (figure not shown), and find a generally similar pattern. However, the positive anomalies in the western coast in the United States are more predominant than those given by *Wallace and Gutzler* [1981]. This is probably due to the difference in seasons and data period used for analysis (April to May for 1982–2000 instead of December to February for 1962–1976). This means there would be an enhanced ridge in that region which would conduct stronger northwesterly air flows to the east of the ridge thus cooling most of the middle and eastern part of the United States. This relationship is confirmed by the temperature changes, as the temperature in Middle North America is correlated with WP at −0.42, and for the whole of North America at −0.51.

[28] The results of linear correlation usually are impacted notably by the outliers. We also investigate what

Table 2. Correlation Between the Atmospheric Circulation Indices and NDVI, Temperature, and the Corresponding Time Coefficients of NDVI and Temperature[a]

	Atmospheric Circulation Index								
	AO	NAO	PNA	EU	SOI	EA	WA	WP	NP
NDVI									
West Siberia	.12	−.20	−.18	**.81**	−.30	**.53**	−.14	−.10	−.27
Middle N. America	**.39**	.34	−.01	−.26	−.19	.20	.01	−.37	.14
East Europe	.04	.05	−.12	.04	**.51**	−.17	−.12	.12	−.01
Northeast Asia	.11	.16	.26	−.00	.13	−.01	−.00	.31	−.09
Northwest N. America	−.18	.36	**.49**	.20	−.32	.16	.17	−.30	**−.57**
North America	.18	.16	.25	−.14	−.35	.16	−.03	**−.42**	−.18
Eurasia	.19	−.06	−.02	**.50**	.08	.34	−.26	.18	−.31
40°−70°N	.23	.01	.10	.33	−.10	.35	−.22	−.05	−.33
Temperature									
West Siberia	.14	−.27	−.26	**.85**	−.24	**.49**	−.00	−.18	−.18
Middle N. America	.35	**.43**	−.08	−.36	−.06	.07	.11	**−.42**	.32
East Europe	−.15	.15	−.11	−.35	**.49**	**−.48**	.07	.26	.32
Northeast Asia	.19	.03	−.01	.35	.33	.17	−.22	**.67**	−.17
Northwest N. America	−.20	**−.41**	**.56**	.24	−.26	.14	.18	−.33	**−.59**
North America	.06	.01	.33	−.29	−.18	.06	.03	**−.51**	−.19
Eurasia	.21	−.10	−.30	**.45**	.23	.18	−.18	.15	.03
40°−70°N	.26	−.09	−.03	.21	.06	.27	−.15	−.24	−.13
Expansion coefficient of NDVI and temperature									
NDVI 1	.06	−.30	−.05	**.72**	−.10	**.42**	−.17	−.01	−.38
Temperature 1	.03	**−.41**	−.04	**.78**	−.17	**.43**	.00	−.06	−.37
NDVI 2	−.26	−.19	−.07	.16	.18	−.16	.12	**.44**	.05
Temperature 2	−.17	−.15	−.08	.26	.12	−.09	.06	**.50**	.01
NDVI 3	.25	.05	−.38	.27	−.34	**.39**	−.06	−.23	.20
Temperature 3	.36	.14	**−.50**	.33	−.22	**.41**	−.20	−.17	.24
NDVI 4	.28	.07	−.05	−.20	.38	.06	−.16	.31	−.06
Temperature 4	.16	.03	−.03	−.31	.36	−.04	−.25	.28	−.03
NDVI 5	.01	.15	**−.56**	−.14	**.52**	**−.40**	−.11	.02	**.50**
Temperature 5	.01	.14	**−.61**	−.19	**.54**	**−.47**	−.11	.07	**.55**
NDVI 6	**.55**	**.52**	−.20	.11	.17	**.47**	−.29	**.55**	.17
Temperature 6	**.56**	**.58**	−0.24	.08	.18	**.45**	−.30	**.59**	.23
NDVI 7	.24	.14	−.15	−.13	.07	−.05	**−.52**	−.05	.11
Temperature 7	.27	.14	−.05	−.02	−.09	.06	**−.56**	−.01	−.01

[a]Correlation coefficients for confidence level of 90%, 95%, and 99% are about ± 0.39, ± 0.46, and ± 0.58, respectively. Significant values are given in bold.

inclusion of the Mount Pinatubo period does to the correlations. The aerosol effects of Mount Pinatubo eruption are noticeable from July 1991 until December 1993. Since we considered only spring season, and the influence is much stronger in 1992 than in 1993, thus we just test the year 1992. We re-calculate the above correlations excluding the data for 1992, and find there is no evident difference in results.

3.5. Time Lag Analysis

[29] It is well-known that the changes in atmospheric circulation may lead variations in surface temperature by several months. The response of vegetation activity to distant atmospheric circulation variations may lag for a certain time. Therefore the simultaneous connection revealed by the above correlation analysis may ignore the most significant correlations between atmospheric circulation and NDVI. We compute the time-lagged correlations for climate indices leading from zero to 6–7 months (i.e., at most half year time lags are considered). Results are shown in Table 3. Clearly, when the time lags are taken into account, more factors show up. For West Siberia, there are 6 climate indices exert significant influence on NDVI with lead times varying from zero to 5 months; in contrast to that, there are only EU and EA two significant factors in nonlagged correlations. For Middle North America NDVI the most significant correlation occurs when WA leads by 5 months, while in the nonlagged correlations the strongest one is for AO. For East Europe NDVI, in addition to SOI there are 4 more climate indices show up. For Northeast Asia there is no significant correlation if no time lags are considered. However, the situation changes much in association with the lagged correlations; three significant indices are found. For Northwest North America, in addition to PNA and NP two more indices (EU and EA) show up. The analysis for temperature, generally speaking, show consistent results. The most significant relations between climate indices and regional NDVI appear also for the temperature. In these cases the lag-time(s) are often close to each other, differences being within 2 months. Of course, there are some exceptions. For some regions only NDVI show significant relations to climate indices, whereas, the temperature does not; and there also some cases in contrast to that. This may be due to the fact that the temperature is not the only climate factor influencing NDVI, and that these nine climate indices are not all atmospheric circulation systems influencing the regional surface climates. For example over the midlatitude to high-latitude Eurasia the Siberian High, the largest anticyclone in boreal cold season, plays important role in recent climate change over there [*Gong and Ho*, 2002;

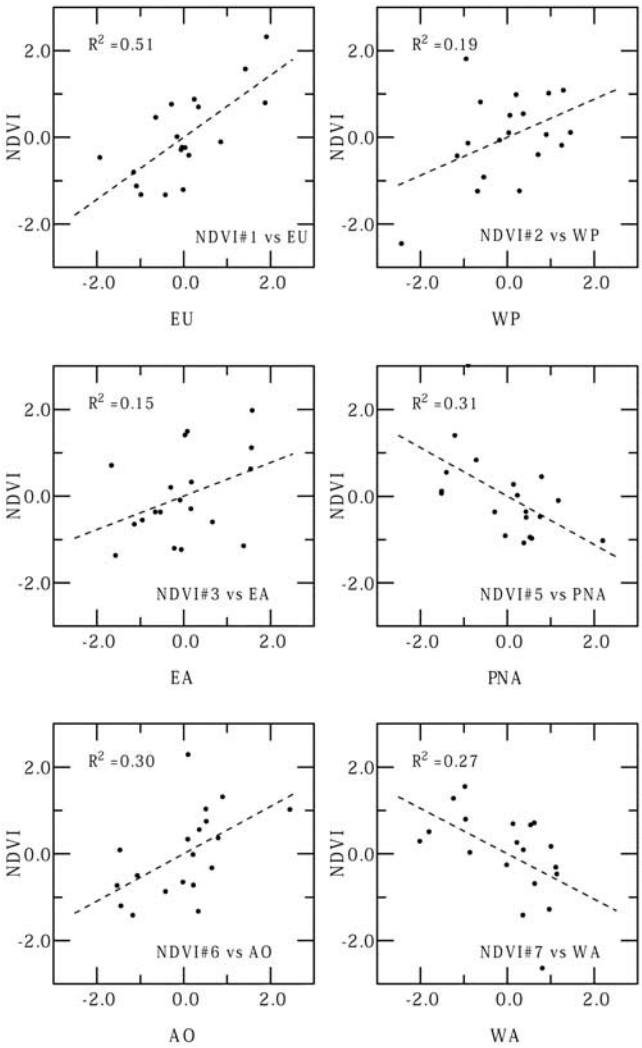

Figure 6. Scatterplots of SVD time coefficients of NDVI against the selected climate indices. Both NDVI time coefficients and atmospheric circulation indices are normalized with respect to the entire period 1982–2000.

Gong and Wang, 1999]. However, it is not considered in the present study.

3.6. NDVI Variance Accounted for by Large-Scale Climate Indices

[30] Some indices show strong connection among them; for example, NP correlates significantly with SOI at 0.5. This implies that in some circumstances a notable proportion of variance in NDVI could be related to more than one atmospheric circulation system. In some other regions, despite the absence of notable, simultaneous correlation existing between NDVI and each single atmospheric circulation index, the correlation become significant when the time lag was taken into account. In order to better understand the NDVI–large-scale climate relation we need to take all these atmospheric circulation systems and the possible time lags into account. Here we apply the stepwise regression analysis to investigate this problem. Moving means of 2 consecutive months from the previous October to April for 9 indices are computed first, then the significant terms among all 63 potential variables (7 time lags $\times$ 9 indices = 63) are considered. We perform an ordinary forward selection and backward elimination screening. The criteria for selection and elimination are both 95% confidence level using a F-test. This method establishes a quantitative relationship between these climate indices and the response, NDVI. Once the significant factors are selected and their quantitative relations with NDVI are determined, we apply it to calculate the climate index-related NDVI. The variance is then estimated and compared with that of the observation.

[31] Figure 7 shows the percent variance of NDVI explained by significant climate indices. Obviously, over most midlatitude to high-latitude North America and Eurasia more than half the variance would be related to the fluctuations in large-scale atmospheric circulation systems. In about 75% of the cells the explained variance is in excess of 50%. Low-value cells are generally located in the arid, semi-arid, and sub-polar regions. Averaging over all calculated cells, the mean value of the explained variance is 71.0%.

[32] As we have shown in the previous sections, in addition to year-to-year variations there are also considerable trends in

Table 3. Month(s) of Atmospheric Indices Leading Spring NDVI When the Maximum Correlation Exists[a]

	AO	NAO	PNA	EU	SOI	EA	WA	WP	NP
Regional mean NDVI and (temperature)									
West Siberia		2(2)	2(1)	0(0)	3		3		5(6)
Middle N. America				(1)			5(5)	(1)	
East Europe	3	3(4)			0(0)	6			4
Northeast Asia	3	3(5)				6(5)	(3)	(0)	
Northwest N. America		(3)	0(0)	5(4)		3			0(0)
N.America				5(5)			5(5)	(0)	
Eurasia	2(2)	3(2)	3	0	5	6(6)	3(5)		5(5)
40–70°N	2	3(3)				3	3		5(5)
Expansion coefficients for NDVI and (temperature)									
Mode 1	2(2)	2(2)		0(0)		(1)	3(5)		5(6)
Mode 2				5(5)			5(5)	(1)	
Mode 3	3(3)	3(3)	(1)						(1)
Mode 4	6(6)							2(2)	(6)
Mode 5			0(0)	(4)	1(1)	(0)			0(0)
Mode 6	0(0)	0(0)	4(4)			6(6)	3(3)	0(0)	3(3)
Mode 7	(5)	1(1)		3(3)		(4)	0(0)	3	

[a]Here, "0" means no leading time, "1" means that the atmospheric indices leads by 1–2 months, "2" by 2–3 months, and so on. Only significant (at 95% level) relationships are presented. Values shown in parentheses are for temperatures.

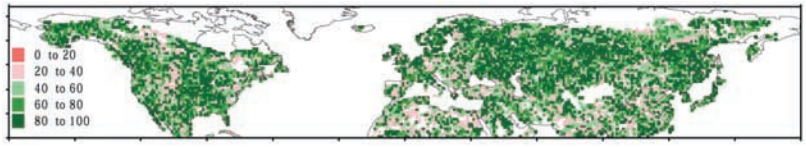

Figure 7. NDVI variance (%) explained by nine climate indices in April–May.

NDVI. To what extent are the trends related to the atmospheric circulation fluctuations? Using the results from the stepwise regression analysis, we also estimate the NDVI trends in association with these atmospheric circulation systems. The results are presented in Figure 8. The trends in observation and residuals are also presented for comparison. The main features in observed and climate-index-related trends are clearly comparable in both their magnitude and spatial distribution. Some regions, including northwestern North America, southeastern North America, most of Europe, Siberia, and East Asia, show the strongest positive trends, and most of these trends would be related to the atmospheric circulations. Besides these positive trend centers, the notable downward trends in northern Scandinavia are also manifest in both the observational and multiple regression results. Averaging over all cells, the mean trend is 0.02243 NDVI/10 years in observation. For the climate-index-related changes the trend is 0.01382 NDVI/10 years. This suggests that at least 61.6% of the trends may be related to the large-scale atmospheric circulation, implying that these circulation systems play essential roles in long-term vegetation changes.

[33] It should be noted that although a large portion of the long-term changes can be explained, there are still considerable residual trends in some midlatitude to high-latitude regions, particularly in a broad zone extending from middle Europe to the western Siberia. Averaging over all cells, the mean trend in residuals is 0.0086 NDVI/10 years. However, what is responsible for the remaining portion of as much as 38.4% of the satellite-sensed trends is still an open question. Local environmental parameters and/or human activity (in some regions such as eastern China and northern Africa) may play important roles in this.

4. Discussion

4.1. Influence of the NDVI Resolution on NDVI-Temperature Relations

[34] The NDVI has much higher spatial and temporal variability than does temperature. This point is important when considering the NDVI-large-scale climate relationship. Compared to the temperature data sets used here (5° resolution), the resolution of NDVI is very different. As we know, the results from spatially oriented techniques are dependent on the data samples in the space domain. Will the NDVI/-temperature relationships change when the NDVI data sets with different resolution are employed?

[35] We have investigated the possible influence of different resolution on the results.The subset of NDVI at the resolutions of $2 \times 2°$, $3° \times 3°$, $4 \times 4°$, and $5° \times 5°$ are respectively tested. Our investigation shows that the above mentioned NDVI/-temperature relationships are stable irrespective of what resolution NDVI is used. The explained co-variances do not change much as the spatial samples drop significantly from $1 \times 1°$ to $5° \times 5°$ (see Table 4). Although the changed samples would impact the singular vectors in values, the corresponding spatial patterns keep very similar features. The anomalous centers, in terms of their locations and relative strength, do not change very much. Figure 9 presents examples of the first NDVI modes for $3° \times 3°$ and $5° \times 5°$. As compared to $1° \times 1°$, the patterns are almost identical. The same is true for the other

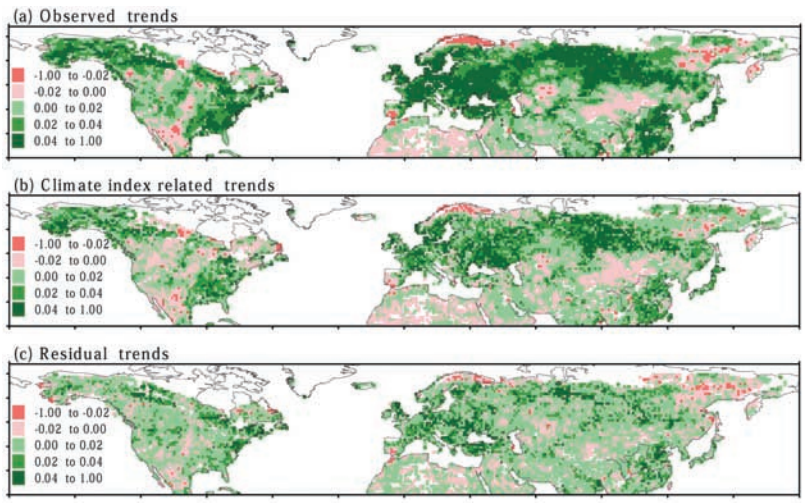

Figure 8. Satellite-sensed NDVI trends (uppermost panel), climate-index-associated NDVI trends (middle panel), and the residual trends (lowest panel). Unit: NDVI/10yr.

Table 4. Squared NDVI-Temperature Covariance Explained by the Leading Seven Singular Values[a]

	NDVI Resolution				
	1° × 1°	2° × 2°	3° × 3°	4° × 4°	5° × 5°
Mode 1	42.6	42.3	42.6	43.4	41.9
Mode 2	19.5	19.7	19.7	19.2	19.5
Mode 3	10.3	10.3	10.6	9.8	10.8
Mode 4	7.7	7.7	7.7	8.1	7.4
Mode 5	5.0	5.1	4.9	4.9	5.3
Mode 6	4.2	4.2	4.1	4.0	4.2
Mode 7	2.3	2.3	2.3	2.5	2.3
Total	91.6	91.6	91.8	91.9	91.4

[a]Covariances are given in percent. Shown are the results from different NDVI resolutions.

NDVI resolutions, as well as for the second to seventh modes. Our results reveal that the large-scale NDVI-temperature connections are independent of the NDVI resolution (at least for 1 to 5 degree resolutions). The time coefficients also keep nearly same features. For example, Figure 10 shows the time coefficients of the modes 1 for 1 degree and 5 degrees, they correlate at 0.99. This also confirms that the regional NDVI changes are inherently associated with the consistent temperature variations.

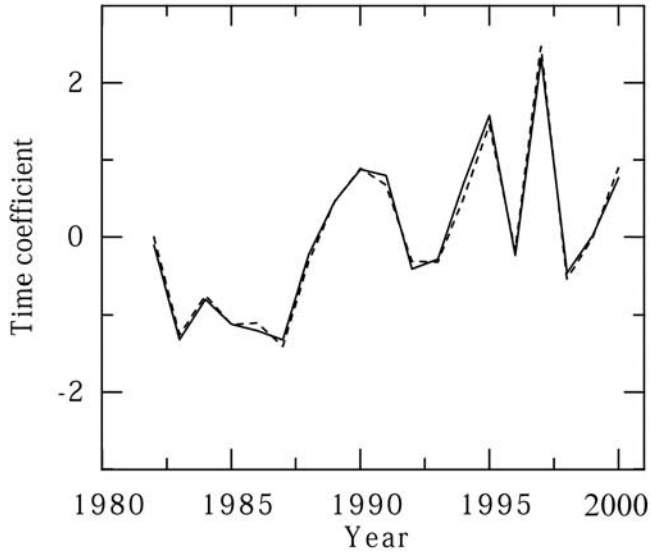

Figure 10. NDVI time coefficients for mode 1. Solid line is the results from the 1 degree resolution data, dashed line from 5 degree NDVI data. Both normalized.

4.2. Influence of ENSO on NDVI

[36] It is widely known that ENSO is the largest signal in the interannual climate variation over the globe [e.g., *Glantz et al.*, 1991; *Wang et al.*, 1999]. ENSO-related precipitation and temperature changes are primarily significant in the tropics [*Ropelewski and Halpert*, 1987, 1996]. Therefore the consequent vegetation response prevails in the lower latitude regions, for instance, the Brail, Indonesia, Australia, and so on. Compared to the tropics, the ENSO influence is weak in midlatitudes to high latitudes. In recent years, numerous studies have investigated the ENSO's impact on NDVI for special tropical regions as well as the entire globe [e.g., *Myneni et al.*, 1996; *Mennis*, 2001; *Kogan*, 2000; *Gutman et al.*, 2000; *Anyamba et al.*, 2001]. Much evidence shows that a stable ENSO-NDVI relationship exists primarily at low latitudes. Contrast to that, the connection is weak over midlatitudes and high latitudes. For example, *Li and Kafatos* [2000] reported that there are evident ENSO signals in the United States vegetation condition (NDVI); however, this signal ranks only as the fifth component loading in their principal components analysis and explained much less of the NDVI variance. Furthermore, in the southeastern United States the ENSO-vegetation relationships were reported as not matching the ground observations [*Kogan*, 2001]. These studies suggest that in the midlatitudes to high latitudes the response of vegetation to ENSO would generally be weak and the relationship would be distorted by the strong midlatitude to high-latitude climate changes.

[37] It should be mentioned that the SOI does not show up in several areas known to be influenced by ENSO in other studies (e.g., western United States and East Asia) and does show up in areas where ENSO effects are hardly noticeable according to the reports of previous studies (e.g., Europe). Among all regions analyzed above, only eastern Europe (Region C) shows a significant relationship with SOI, $r = 0.51$, which means that during the El Niño years the NDVI there would tend to decrease. The NDVI for other regions as well as the two continents and the northern hemispheric mean show no significant correlation with SOI; neither does the temperature. Even when the time lags are considered, among 5 regions only West Siberia shows significant correlations to SOI with 3 months

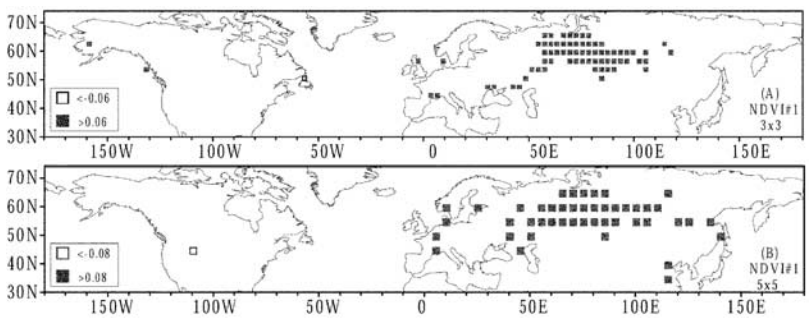

Figure 9. First NDVI mode from the SVD analysis for resolutions of 3° × 3° and 5° × 5°. Please note that only the maximum and minimum values are shown to highlight the anomalous centers. Less space samples result in higher absolute values of singular vectors, therefore different thresholds are used here.

Table 5. Squared NDVI-Temperature Covariance Explained by the Leading Seven Singular Values[a]

	0.3σ	0.5σ	0.3σ + 0.5σ	Detrended
Mode 1	41.3	39.6	40.8	40.3
Mode 2	19.3	18.8	19.1	17.0
Mode 3	10.4	10.4	10.1	12.8
Mode 4	7.8	7.9	7.9	7.5
Mode 5	5.1	5.4	5.4	6.0
Mode 6	4.3	4.4	4.4	3.5
Mode 7	2.5	2.7	2.5	2.9
Total	90.7	89.2	90.2	90.1

[a]Covariances are given in percent. Shown are the results from the "contaminated" NDVI data sets which are generated by superimposing random errors upon the original data. Here the added errors have different standard deviations, "0.3σ" means at each pixel the random error with 0.3σ of original NDVI has been superimposed for the whole period. "0.5σ" means the error is 0.5σ. "0.3σ + 0.5σ" means that 0.3σ error has been added for period 1982–1991, and 0.5σ error for period 1992–2000. "Detrended" means that the linear trend in NDVI has been removed before analysis.

lead time; but at the same time there is no significant connection found for temperature. Such might result from several causes. First, the ENSO influence is of strong seasonality. For example, over East Asia the ENSO impact is most significant in autumn and winter. Second, in the present study we consider only temperature, whereas some well-known ENSO influence in some regions is most significant for precipitation. In some circumstances such as in the semi-arid areas, the precipitation would play a key role in the vegetation activity [*Kawabata et al.*, 2001; *Suzuki et al.*, 2000]. There is possibility that some addressed ENSO signals may be due to the influence of precipitation, as well as (or instead of) temperature.

4.3. Possible Influence of Pathfinder Data Errors on NDVI-Temperature Relations

[38] There is no perfect data set available at present for representing NDVI. There are errors in Pathfinder NDVI data set resulting from cloud effects, volcanic aerosol effects, etc. Many studies are given to the improvement of the data quality [e.g., *Los*, 1993, 1998]. No matter how great the effort made in physical or computational aspects, the NDVI data, to some degree, still contain errors. Here we do not try to correct the raw data errors. Rather, we test the possible influence of the NDVI errors on the NDVI-temperature relations by intentionally superimposing errors upon the original NDVI data. Here two possible forms of errors are considered: first, we check the possible influence of error with different magnitudes. We compare the results from contaminated NDVI data with error standard deviations (σ) of 0.3σ and 0.5σ (0.3σ means the errors' standard deviation is 0.3 times that of the original NDVI time series at each pixel); second, we check the possible influence of discontinuous errors by adding different errors for different periods, 0.3σ errors added for period 1982–1991 and 0.5σ errors added for 1992–2000. Results are shown in Table 5. As the errors increase the explained covariance between NDVI and temperature decrease, but the drop is not remarkable with the errors getting as large as even half of the original NDVI standard deviation. In addition, the corresponding spatial modes are almost identical to the results from the original data sets; and the expansion coefficients are also correlated with those from the original data sets at very high values. When 0.3σ errors are superimposed upon the original NDVI data, the correlations between contaminated and original data for each mode vary in the range 0.98–0.99. The same is true for the 0.3σ-error case. Clearly, the real errors should be larger than these values since the original NDVI data used here have already been contaminated by errors. The analysis implies that the NDVI-temperature coupling modes revealed by SVD analysis are stable and detectable even when there are remarkable errors in the original NDVI data sets.

[39] In addition to the above mentioned kinds of errors, the NDVI data often contain another kind of error, the trend. To check the extent to which the possible error trend affect the results, a test is also carried out using the detrended NDVI. Results show that the removal of NDVI trends do not affect the major features of the leading modes (see Table 5). Correlation between the nondetrended time coefficient 1 and the detrended one is 0.75, spatial correlation for the modes 1 is 0.91. Correlations for the second time coefficients and modes are 0.70 and 0.70; for the 3rd time coefficients and modes, are 0.92 and 0.90, respectively. However, it is noted that time coefficient 1 for nondetrended NDVI shows a significant upward trend, but the result from detrended NDVI does not. Therefore we should caution that the trends caused by errors might affect the long-term features in the temporal characteristics of the modes. It should be mentioned that here we do not separate the error induced trends from the real long-term changes. Some error corrected NDVI data suggested a significant strong spring NDVI trend that is almost identical to the value calculated from the uncorrected AVHRR NDVI data as shown in the present work [cf. *Zhou et al.*, 2001]. Here we assumed that the error-related trends might not be important in comparison to the real long-term changes.

5. Concluding Remarks

[40] The NDVI-temperature relationship revealed in the present study is robust and does not change significantly when the NDVI was rescaled from 1 to 5 degrees. The SVD method is an appropriate and powerful technique for detecting the vegetation-climate relationship.

[41] The NDVI changes in response to temperature fluctuations on the interannual timescale show well-defined large-scale and consistent patterns. The leading paired modes indicate that the most significant association between vegetation and temperature is located in western Siberia, implying that there is sensitive and enhanced bioactivity in association with profound temperature warming during the last two decade in the spring season. This coupled mode is the most important. The large-scale atmospheric system, EU, plays a dominant role in that.

[42] Much of the NDVI-temperature covariance can be related to the fluctuations in several important large-scale atmospheric circulation systems. Averaging over the mid-latitude to high-latitude Northern Hemisphere, 71.0% of the satellite-sensed NDVI variance is explained by nine atmospheric systems. The nine climate indices with time lags taken into account can explain a large portion of the long-term trends in NDVI too, particularly in northwestern North America, southeastern North America, most of Europe,

Siberia, and East Asia. On average, the climate-index-related trend is 0.01382 NDVI/10 years, implying that at least 61.6% of the observed trends may be associated with the large-scale climate systems.

[43] Future global climate change scenarios indicate considerable changes in atmospheric circulation variability. This implies that the regional response of vegetation to climate fluctuations under these scenarios would differ from region to region. Some areas related to the important circulation systems would experience higher sensitivity and predominant changes than other regions.

[44] **Acknowledgments.** The first author was supported by the NKBRSF Project under grant G2000018604 and by the Huo Ying-Dong Education Foundation Program-81014. This study was performed for the project Technical Development for Remote Sensing Meteorology, one of the Research and Development programs on Meteorology and Seismology funded by the Korea Meteorological Administration (KMA). Data used in this study include data produced through funding from the Earth Observing System Pathfinder Program of NASA's Mission to Planet Earth in cooperation with NOAA. The NDVI data were provided by the Earth Observing System Data and Information System, Distributed Active Archive Center, at Goddard Space Flight Center, which archives, manages, and distributes this data. Thanks are due to the anonymous reviewers for their constructive comments on the early version of this manuscript.

References

Agbu, P. A., and M. E. James, The NOAA/NASA Pathfinder AVHRR land data set user's manual, http://xtreme.gsfc.nasa.gov/, Goddard Distrib. Active Arch. Cent., NASA Goddard Space Flight Cent., Greenbelt, Md., 1994.

Anyamba, A., C. J. Tucker, and J. R. Eastman, NDVI anomaly patterns over Africa during the 1997/98 ENSO warm event, *Int. J. Remote Sens.*, *22*, 1847–1859, 2001.

Barber, V. A., G. P. Juday, and B. P. Finney, Reduced growth of Alaska white spruce in the twentieth century from temperature-induced drought stress, *Nature*, *405*, 668–672, 2000.

Bogaert, J. L., L. Zhou, C. J. Tucker, R. B. Myneni, and R. Ceulemans, Evidence for a persistent and extensive greening trend in Eurasia inferred from satellite vegetation index data, *J. Geophys. Res.*, *107*(D11), 4119, doi:10.1029/2001JD001075, 2002.

Bretherton, C. S., C. Smith, and J. M. Wallace, An intercomparison of methods for finding coupled patterns in climate data, *J. Clim.*, *5*, 541–560, 1992.

Glantz, M. H., R. W. Katz, and N. Nicholls (Eds.), *Teleconnections Linking Worldwide Climate Anomalies*, 535 pp., Cambridge Univ. Press, New York, 1991.

Gong, D. Y., and C. H. Ho, Siberian High and climate change over middle to high latitude Asia, *Theor. Appl. Climatol.*, *72*, 1–9, 2002.

Gong, D. Y., and S. W. Wang, Long-term variability of the Siberian High and the possible influence of global warming, *Acta Geogr. Sin.*, *54*(2), 125–133, 1999.

Gutman, G., I. Csiszar, and P. Romanoc, Using NOAA/AVHRR products to monitor El Niño impact: Focus on Indonesia in 1997–98, *Bull. Am. Meteorol. Soc.*, *81*, 1189–1204, 2000.

Hurrell, J. W., Decadal trends in the North Atlantic Oscillation: Regional temperatures and precipitation, *Science*, *269*, 676–679, 1995.

Hurrell, J. W., Influence of variations in extratropical wintertime teleconnections on Northern Hemisphere, *Geophys. Res. Lett.*, *23*, 665–668, 1996.

Intergovernmental Panel on Climate Change (IPCC), *Climate Change 2001: The Scientific Basis, Contribution of Working Group I to the Third Assessment Report of the Intergovernmental Panel on Climate Change*, edited by J. T. Houghton et al., 881 pp., Cambridge Univ. Press, New York, 2001.

James, M. E., and S. N. V. Kalluri, The Pathfinder AVHRR land data set: An improved coarse-resolution data set for terrestrial monitoring, *Int. J. Remote Sens.*, *15*, 3347–3364, 1994.

Jones, P. D., Hemispheric surface air temperature variations: A reanalysis and an update to 1993, *J. Clim.*, *7*, 1794–1802, 1994.

Kawabata, A., K. Ichii, and Y. Yamaguchi, Global monitoring of interannnual changes in vegetation activities using NDVI and its relationships to temperature and precipitation, *Int. J. Remote Sens.*, *22*, 1377–1382, 2001.

Keeling, C. D., J. F. S. Chin, and T. P. Whorf, Increased activity of northern vegetation inferred from atmospheric CO_2 measurements, *Nature*, *382*, 146–149, 1996.

Kogan, F. N., Satellite-observed sensitivity of world land ecosystems to El Niño/La Niña, *Remote Sens. Environ.*, *74*, 445–462, 2000.

Kogan, F. N., Operational space technology for global vegetation assessment, *Bull. Am. Meteorol. Soc.*, *82*, 1949–1964, 2001.

Li, Z. T., and M. Kafatos, Interannual variability of vegetation in the United States and its relation to El Niño/Southern Oscillation, *Remote Sens. Environ.*, *71*, 239–247, 2000.

Los, S. O., Calibration adjustment of the NOAA-AVHRR normalized difference vegetation index without recourse to component channel 1 and 2 data, *Int. J. Remote Sens.*, *14*, 1907–1917, 1993.

Los, S. O., Estimation of the ratio of sensor degradation between NOAA AVHRR channel 1 and 2 from monthly NDVI composites, *IEEE Trans. Geosci. Remote Sens.*, *36*, 202–213, 1998.

Los, S. O., G. J. Collatze, L. Bounoua, P. J. Sellers, and C. J. Tucker, Global interannual variations in sea surface temperature and land surface vegetation, air temperature, and precipitation, *J. Clim.*, *14*, 1535–1549, 2001.

Mennis, J., Exploring relationships between ENSO and vegetation vigour in the southeast USA using AVHRR data, *Int. J. Remote Sens.*, *22*, 3077–3092, 2001.

Myneni, R. B., S. O. Los, and C. J. Tucker, Satellite-based identification of linked vegetation and sea surface temperature anomaly areas from 1982–1990 for Africa, Australia, and South America, *Geophys. Res. Lett.*, *23*, 729–732, 1996.

Myneni, R. B., C. J. Tucker, G. Asar, and C. D. Keeling, Interannual variations in satellite-sensed vegetation index data from 1981 to 1991, *J. Geophys. Res.*, *103*(D6), 6145–6160, 1998.

Myneni, R. B., J. Dong, C. J. Tucker, R. K. Kaufmann, P. E. Kauppi, J. Liski, L. Zhou, V. Alexeyev, and M. K. Hughes, A large carbon sink in the woody biomass of northern forests, *Proc. Natl. Acad. Sci. U. S. A.*, *98*, 14,784–14,789, 2001.

Ropelewski, C. F., and M. S. Halpert, Global and regional scale precipitation patters associated with El Niño/Southern Oscillation, *Mon. Weather Rev.*, *115*, 1606–1626, 1987.

Ropelewski, C. F., and M. S. Halpert, Quantifying Southern Oscillation precipitation relationships, *J. Clim.*, *9*, 1043–1059, 1996.

Suzuki, R., S. Tanka, and T. Yasunari, Relationships between meridional profiles of satellite-derived vegetation index (NDVI) and climate over Siberia, *Int. J. Climatol.*, *20*, 955–967, 2000.

Tans, P. P., I. Y. Fung, and T. Takahashi, Observations on the global atmospheric CO_2 budget, *Science*, *247*, 1431–1438, 1990.

Thompson, D. W. J., and J. M. Wallace, The Arctic Oscillation signature in the wintertime geopotential height and temperature fields, *Geophys. Res. Lett.*, *25*, 1297–1300, 1998.

Thompson, D. W. J., J. M. Wallace, and C. Gabriele, Annular modes in the extratropical circulation, Part II: Trends, *J. Clim.*, *13*, 1018–1036, 2000.

Trenberth, K. E., and J. W. Hurrell, Decadal atmosphere-ocean variations in the Pacific, *Clim. Dyn.*, *9*, 303–319, 1994.

Tucker, C. J., and P. J. Sellers, Satellite remote sensing of primary production, *Int. J. Remote Sens.*, *7*, 1395–1416, 1986.

Tucker, C. J., D. A. Slayback, J. E. Pinzon, S. E. Los, R. B. Myneni, and M. G. Taylor, Higher northern latitude normalized difference vegetation index and growing season trends from 1982 to 1999, *Int. J. Biometeorol.*, *45*, 184–190, 2001.

Wallace, J. M., and D. S. Gutzler, Teleconnections in the geopotential height field during the Northern Hemisphere winter, *Mon. Weather Rev.*, *109*, 84–812, 1981.

Wallace, J. M., C. Smith, and C. S. Bretherton, Singular value decomposition of wintertime sea surface temperature and 500-mb height anomalies, *J. Clim.*, *5*, 561–576, 1992.

Wang, H. J., R. H. Zhang, J. Cole, and F. Chavez, El Niño and the related phenomenon Southern Oscillation (ENSO): The largest signal in interannual climate variation, *Proc. Natl. Acad. Sci. U. S. A.*, *96*, 11,071–11,072, 1999.

Zhou, L. M., C. J. Tucker, R. K. Kaufmann, D. Slayback, N.V. Shabanov, and R. Myneni, Variations in northern vegetation activity inferred from satellite data of vegetation index during 1981 to 1999, *J. Geophys. Res.*, *106*(D17), 20,069–20,083, 2001.

D.-Y. Gong, Key Laboratory of Environmental Change and Natural Disaster, Institute of Resources Science, Beijing Normal University, 100875 Beijing, China. (gdy@pku.edu.cn)

C.-H. Ho, School of Earth and Environmental Sciences, Seoul National University, San 56-1 Shinlim-dong, Kwanak-ku, Seoul 151–742, Korea. (hoch@cpl.snu.ac.kr)